EURASIP Journal on Wireless Communications and Networking
a SpringerOpen Journal

RESEARCH Open Access

60 GHz ultra-wideband channel estimation based on a cluster sparsity compressed sensing

Xuebin Sun*, Yuhang Jia, Meng Hou and Chenglin Zhao

Abstract

The propagations of 60 GHz millimeter-wave system, which occupies an enormous operation bandwidth, are always known to be intensively dispersive. This may, in practice, pose great challenges to the estimation of channel state information. In this article, we investigated a promising compressed sensing (CS) algorithm and its practical applications in the channel estimations of emerging 60 GHz millimeter-wave communications. By fully considering the particular characteristics of 60 GHz propagations and further utilizing another kind of channel sparsity, i.e., the specific block cluster sparsity embodied by the identified multiple clusters, a novel cluster sparsity compressed sensing (CS-CS) algorithm is proposed subsequently. Based on the provided experimental simulations, the comprehensive analysis on both the classical regularized orthogonal matching pursuit algorithm and our newly designed CS-CS algorithm are conducted. As has been demonstrated, the proposed new algorithm indeed shows a much superior performance compared with the other existing methods, which may significantly reduce the reconstruction error and hence improve the precision of channel estimation. At the same time, the time complexity of signal reconstruction of the new CS-CS algorithm may be simplified to some extent.

Keywords: 60 GHz millimeter-wave, Compressed sensing, Channel estimations, Cluster sparsity, Cluster sparsity compressive sensing

1 Introduction

The growing demands for high-speed data streams and broadband wireless services have significantly driven the worldwide researches on 60 GHz millimeter-wave frequency band communications, which is mainly designed for the wireless accessing network such as the pico-cellular mobile systems, the wireless local area networks (WLANs), and wireless personal area networks (WPANs) [1]. In order to achieve the targeted ultra-high throughput in the next generation WLAN systems, which may typically even surpass 1 Gbps to provide online uncompressed high-definition television or UHDTV and gigabits per second (Gbps) Ethernet, the new WLAN/WPAN standards are currently developed by the IEEE 802 standardization committee. Two related standards for the short-range indoor applications, i.e., IEEE802.11.TG ac and IEEE802.11.TG ad [2], are designed to operate in different frequency bands less than 6 and 60 GHz, respectively. The main motivation for 60 GHz millimeter-wave communications is the availability of abundant unauthorized spectrum resources, which enables the realization of Gbps transmission as well as the worldwide broader market of 60 GHz products and therefore attracts a large number of famous manufacturers.

Accordingly, with this enormous signal bandwidth, the multi-gigabit capacities and low latency transmissions can be practically promised by the 60 GHz millimeter-wave communication systems. Nevertheless, the emission bandwidth of one single physical layer channel may even approach 2.16 GHz in order to support the high data rate transmissions [3]. Consequently, such a huge bandwidth may significantly enhance the time resolution of 60 GHz receivers (typically in a nanosecond level). Further taking the indoor seniors into considerations, which may usually involve many obstructions (e.g., desks, walls), then the 60 GHz channel is always known to be dispersive into dozen of resolvable multipath [4]. Thus, in order to effectively capture the multipath energy in receivers, the channel estimation has been considered as a key research field in 60 GHz communications. Unfortunately, in sharp contrast to the traditional narrow-band systems, channel estimation in 60-GHz millimeter-wave

* Correspondence: sunxuebin@bupt.edu.cn
Key Lab of Universal Wireless Communications, MOE, Beijing University of Posts and Telecommunications, Beijing 100876, People's Republic of China

systems is supposed to recover so many (e.g., tens of) resolvable multipath components (MPCs) that it may easily become infeasible in practice, given the computationally complicated estimation algorithm and the impractically ultra-high sampling frequency.

Emerging as an extremely powerful technique in modern signal processing, compressed sensing (CS) enables a more promising acquisition of realistic signals at a competitive sampling rate, which is much lower than the previously widely suggested Nyquist sampling rate. In order to implement such performance, CS essentially accomplishes the signal sensing as well as signal compression via an unfired single task [5]. With an appealing sparsity processing framework, CS focuses essentially on the signal sparsity which can be observed in any domain, e.g., time domain, frequency domain, and wavelet domain. It has been commonly recognized that a sparse signal can be recovered with the high probability, by only relying on a set of random linear projections of input signals and using certain nonlinear reconstruction or optimization algorithms [6]. As a consequence, the number of random measurements required in CS is often dramatically smaller than the number of samples required in the other existing Nyquist sampling methods, which thereby leads to a significantly reduced sampling rate and hence greatly alleviate the complicated high-rate analog-to-digital converter (ADC).

More and more experiments have indicated the particularly sparse characteristics of wireless propagation channels, especially for the systems with enormous bandwidth. That is, less than 10% of resolvable multipath component dominated more than 85% of the whole channel energy, and the sparse characteristics of 60 GHz millimeter-wave channels may become much more remarkable in practice [7]. Therefore, CS is regarded as a promising tool to conduct channel estimations, which may acquire and recover the sparse signal at less than the Nyquist sampling rate. However, it is noted that in the application of CS into the channel estimation of 60 GHz communication systems, the signal reconstruction algorithm may also have an important influence on the recovery performance (e.g., the recovery precision) [8]. In other words, different algorithms may have quite different performances. As suggested by our investigation, the classical orthogonal matching pursuit (OMP) algorithm and regularization orthogonal matching pursuit (ROMP) algorithm may be properly introduced to 60 GHz channel estimation. But the performance is still far from unsatisfactory, considering the resulting high recovery error and complexity.

We may notice that from the 60 GHz millimeter-wave channels that are dramatically different from the narrow-band systems, except for the overall sparsity of channel MPCs that attenuated by following an exponent decay function, the local sparse property introduced by the cluster phenomenon may greatly facilitate the practical designs of efficient reconstruction algorithm [9]. Based on the cluster identification results, the local sparsity can be observed, i.e., the few nonzero coefficients occurring in each cluster, which may be referred to as the block cluster sparsity. By explicitly taking such specific block structures into account, both in terms of the recovery algorithm and in terms of the measure that are used to characterize the performance, a novel cluster sparsity compressive sensing (CS-CS) algorithm for 60 GHz channel estimation is proposed. The reconstruction performance (i.e., reconstruction error and iterative convergence) is compared with the classical ROMP algorithms based on the extensive experimental simulations. It has been shown that the proposed CS-CS algorithm can significantly enhance the accuracy of 60 GHz channel estimations, and simultaneously exhibits a much faster iteration behavior. The advantage of such a new CS-CS may be essentially attributed to the full exploitation the specific cluster sparsity, except for the overall sparsity as in conventional sense.

The remainder of this paper is organized as follows. In Section 2, we discussed 60 GHz channeling model and briefly introduced the classical CS theory. In Section 3, we analyze the block sparsity embodied by the multiple clusters, and on this basis, the more competitive cluster sparsity-based compressed sensing algorithm for the channel estimations of 60 GHz millimeter-wave is developed. In Section 4, the comprehensive experimental simulations and comparative performance analysis are provided. Finally, we conclude the whole investigation in Section 5.

2 System model

2.1 60 GHz Channel modeling

In this article, we consider the channel modeling approved by the IEEE802.15.3c TG (i.e., the next-generation WLAN standard at 60 GHz band) [10], which is originally developed for indoor communications and also known as the Saleh-Valenzuela (S-V) channel modeling, to characterize the wireless propagations of 60 GHz millimeter-wave short-range communications. Attributed to the enormous emission bandwidth (typically surpassing 2 GHz) and the resulting fair time resolution as well as the many involved objects in operating environments, the 60 GHz propagation is always an intensive multipath channel, which also assumes the received resolvable MPCs arrive in clusters. That is, the rays within a cluster (or a group) may have independent phases as well as independent amplitudes distribution whose variances decay exponentially with cluster and rays delays.

The popular mathematic formulation for the channel impulse response (CIR) of the cluster-based 60 GHz channel can be expressed as follows:

$$h(t) = \sum_{l=0}^{L} \sum_{m=-M_b}^{M_f} \alpha_l \beta_m \sigma(t - T_l - \tau_{lm}), \quad (1)$$

where the inter-cluster amplitude can be described by

$$|\beta_{lm}^2| = \begin{cases} \exp(\tau_{lm}/\gamma_-) & \tau_{lm} < \tau_{l0} \\ \exp(\tau_{lm}/\gamma_+) & \tau_{lm} > \tau_{l0} \end{cases}. \quad (2)$$

The arrival time of the rays in two side of each cluster may follows the Poisson distribution, i.e.,

$$P(\tau_{l(m-1)}|\tau_{lm}) = \lambda_- \exp[-\lambda_-(\tau_{lm} - \tau_{l(m-l)})], \quad m < 0 \quad (3)$$

$$P(\tau_{lm}|\tau_{l(m-1)}) = \lambda_+ \exp[-\lambda_+(\tau_{lm} - \tau_{l(m-l)})], \quad m > 0, \quad (4)$$

where γ_- and γ_+ represent ray decay parameters, respectively; λ_- and λ_+ account to ray arrival rates which assumed to follow Poisson processes, and m and l denote the index of ray and cluster. M_b and M_f represent the total number of rays for each side in one cluster. The phase of each ray is assumed to be an independent uniform random variable. The α_l, T_l, and L respectively denote the peak power of the lth cluster, the arrival time of the lth cluster, and the total number of clusters.

It has been recognized that the cluster power may also follow an exponential decay rule, and the arrival of clusters follows the Poisson distribution [11]. Thus, we may have

$$|\alpha_l^2| = \exp(-T_l/\Gamma) \quad (5)$$

$$P(T_l|T_{l-1}) = \Lambda \exp[-\Lambda(T_l - T_{l-1})], l > 0, \quad (6)$$

where Γ is the cluster decay parameter, and Λ is the cluster arrival rate which is also assumed to obey the Poisson process.

The simulated 60 GHz millimeter CIRs, for both the line-of-sight (LOS) and non-line-of-sight (NLOS) scenarios in typical short-range indoor applications, have been plotted by Figures 1 and 2, respectively. It is seen that from the simulated CIR in the case of LOS, the amplitude of the first LOS MPC remains usually 15 dB (or even much) higher than that of the second clusters. In other words, the direct wave component may exhibit the largest power and therefore, such strong reflection wave may be observed in the LOS scenario. Meanwhile, the amplitude of the subsequent clusters after the second cluster becomes dramatically lower than that of the second cluster. As a consequence, when the 60 GHz directional transmissions are considered, i.e., the LOS links, ignoring the insignificant clusters whose time of arrival is later than the first three clusters, may become also acceptable for realistic analysis. While from the simulated CIR of NLOS scenario in Figure 2, we may easily note that the first MPC is no longer the highest one, and these NLOS MPCs have been significantly attenuated by the involved obstacles.

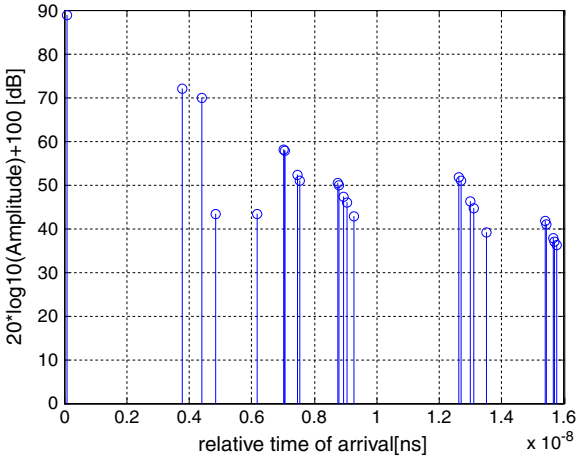

Figure 1 The impulse response of 60 GHz channel for LOS case. Notice that, for illustration, the logarithmic coordinate of multipath amplitude is used.

No matter what kinds of 60 GHz channels are considered, the wireless propagations of 60 GHz millimeter-wave systems may exhibit the unique characteristic of intensive multipath, and therefore, the channel estimation may require capturing dozens of resolvable MPCs. Taking the resulting extremely high sampling rate and the complicated estimation algorithms into account, the traditional channel estimation techniques, which relies essentially on the classical Shannon theorem, may

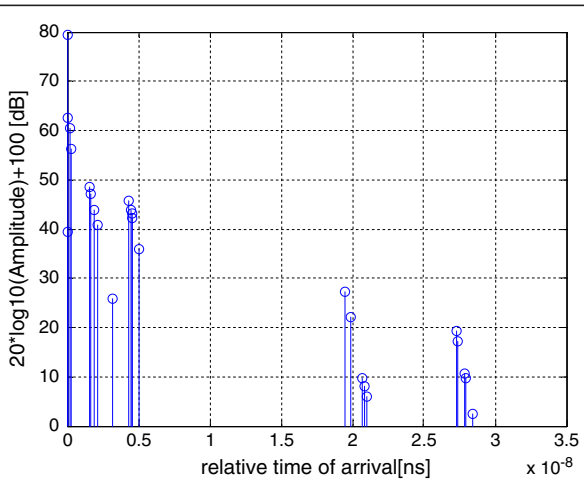

Figure 2 The impulse response of 60 GHz channel for NLOS case. Notice that, for illustration, the logarithmic coordinate of multipath amplitude is used.

become obviously unbearable for the low-rate ADC device and low-complexity implementation.

2.2 Compressed sensing (CS)

In order to avoid the loss of information in the acquisition the input signal, the well-known Shannon/Nyquist sampling theorem has stated that the sampling rate must be configured at least two times faster than the original signal bandwidth [11]. In many applications, such as the storage of digital images and video streams, such a Nyquist rate seems to be still much too high with so many realistic applications so that a preprocessing (i.e., a compression) is usually necessary prior to the storage or transmission. Unfortunately, increasing the sampling rate in the signal capture is rather expensive. As a promising new technique, compressive sensing (CS) may provide a feasibly alternative solution to the above problems, by allowing sampling signals at a rate significantly lesser than the Nyquist rate.

Before proceeding further, we may briefly describe the well-developed CS framework proposed in [12]. Assume $\mathbf{f}$ is an N-point discrete-time sparse signal, and $\mathbf{\Phi}$ is a $K \times N$ measurement matrix, and then we may have

$$\mathbf{f} = \sum_{i=1}^{M} \theta_{l_i} \psi_{l_i} = \mathbf{\Psi\Theta} \tag{7}$$

for $K < < N$. That is, $\mathbf{f}$ can be recovered from the received signal, with high probability as long as the measurement matrix $\mathbf{\Phi}$ remains incoherent with the prescribed dictionary $\mathbf{\Psi}$ [13]. In Equation 7, $\mathbf{\Theta} = [\theta_1, \theta_2, \ldots, \theta_z]^T$ is a column vector which contains M nonzero coefficients. The index of the nonzero coefficient specifies which element in the dictionary composes the signal, and the coefficient measures the contribution (or the weight) of such an element in defining the original signal $\mathbf{f}$ [14].

Based on the above formulation, the signal $\mathbf{f}$ can be then recovered from the solution of Equation 7, via the well-defined convex and non-quadratic optimization problems (i.e., basis pursuit) [13], which finally yields the sparse vector $\mathbf{\Theta}$. With a CS framework with very high probability, $\mathbf{\Theta}$ is the unique solution to

$$\begin{aligned} &\min \|\mathbf{\Theta}\|_{l_1} \\ &s.t \quad \mathbf{y} = \mathbf{V}\mathbf{f}, \end{aligned} \tag{8}$$

where $\cdot_{l_1}$ denotes the l_1 norm, $\mathbf{V} = \mathbf{\Phi\Psi}$ is the holographic dictionary, and $\mathbf{y}$ is the received signal (i.e., observations). It has been shown by [14] that if the random measurement matrix has sufficient entries taken from *a priori* normal distribution and the number of random projection (i.e., K) is greater than or equal to $c_1 M \log_2(N/M)$, then the probability of the exact reconstruction may surpass $(1-e^{c_2 K})$, where c_1 and c_2 are some constants. In other words, it is possible to use the much less samples to reconstruct the original signal by dramatically alleviating the burden in signal acquisition aroused by traditional Shannon/Nyquist sampling theorem, which is hence of great promising to various different realistic applications.

Signal reconstruction algorithm is the core of compressed sensing theory, and it is the process of reconstruction sparse signal $\mathbf{x}$ (length N) by the help of the measurement vector (used $\mathbf{M}$ times). OMP and ROMP algorithms are the most classical solutions for compressed sensing. They both belonged to Greedy algorithm. Moreover, ROMP was derived from OMP, and the idea of normalized orthogonal treatment was introduced into ROMP. Table 1 shows the improved CS-CS algorithm which is not the basis of ROMP.

2.3 CS-based channel estimation

It is no doubt that CS may provide an appealing solution to the above practical difficulties posed by channel estimations with intensive multipath propagations, by allowing sampling the signals (with a huge bandwidth) at a feasible rate significantly lesser than the Nyquist rate [15]. In recent years, extensive investigations have been devoted to such fields, and a variety of CS reconstruction algorithms have been put forward.

Among these, the regularization ROMP algorithm is the most representative one, which has been considered with great interest from both theoretical analysis and applications designing. The ROMP scheme employs the random linear projections, which can basically preserve the structure of input signals that are usually sparse in some basis (e.g., time domain). Based on this formulation, an optimization process is then employed to reconstruct the required signal.

Nevertheless, the ROMP algorithm and the classical CS theoretical framework may still become unacceptable to the considered 60 GHz channel estimations. First, by ignoring the detailed specific structures of 60 GHz multipath channels, the ROMP algorithm may impractically require at least K (K denotes sparsity of signal) iterations in order to reconstruct the original signal, which results in a much higher complexity $O(KMN)$, where M denotes the number of measurements and N denotes the length of the signals. More importantly, the false matches seem to be inevitable in practice when ROMP is applied to realistic channel estimations.

3 CS-CS-based channel estimation

It has been highlighted that the 60 GHz multipath channel is relatively special, which may show quite different characteristics from the other S-V multipath channels (e.g., ultra-wideband channel). To be specific, the power delay profiles (PDP) in LOS situations can be firstly

Table 1 Cluster-sparse compressed sensing

Step	Description/instruction
A	Cluster identification
B	Cluster-based classification
C	If sparsity of primary cluster is greater than threshold, go to step E, otherwise go to step D
D	Extract the primary cluster as the first classification and the rest as the second part, go to F
E	Extract the primary cluster and the second cluster as the first classification and the rest as the second part, go to F
F	Reconstruction
	Input measurement vector $\mathbf{h} \in \square^{N}$; sparsity K
	Initialize index set $\Lambda = \varnothing$ and the residual error $r = h$. Repeat the following steps by K times or until $\lvert\mathbf{\Lambda}\rvert \geq 2K$
	Select the maximum K nonzero values from measurement matrix $\mathbf{u} = \mathbf{\Phi r}$ and insert into index set $\mathbf{j}$
	Regularization: let all subset $\mathbf{j_0} \subset \mathbf{j}$ for all $k, l \in \mathbf{j_0}$ satisfy $u(k) \leq 2\lvert u(l)\rvert$. Then select the index set with a maximum energy as j_0
	Update: add subset $\mathbf{j_0}$ to index set: $\mathbf{\Lambda} \leftarrow \mathbf{\Lambda} \cup \mathbf{j_0}$,update the residual error $\mathbf{r}$:
	$y = \arg\min_{\mathbf{z} \in \mathbb{R}^l} \lVert \mathbf{h} - \mathbf{\Phi z} \rVert_2$, $\mathbf{r} = \mathbf{h} - \mathbf{\Phi y}$
	If the iteration number is greater than K or the number of indexes is greater than 2 K, stop the iteration, otherwise continue the iteration
	Index set: $\mathbf{\Lambda} \subseteq \{1, \ldots d\}$, then reconstruct the signal estimate as $v = y$
G	Signal synthesis

divided into two independent parts, i.e., the direct wave component (or the first path) and the remaining strong reflection waves [15]. Usually, the first path can be modeled by a simple impulse response. Meanwhile, the other strong reflection components can be formed into a cluster shape in the time domain. Although the direct wave component has vanished in NLOS cases, similarly, these NLOS paths also show relatively predominant cluster property.

Furthermore, it may be note worthy that from the simulation results shown in Figure 1 and Figure 2, the simulation CIRs can be regarded to a special channel with two-level sparsity. That is, both *inter-cluster* and *intra-cluster* models may exhibit the sparse characteristics. By fully exploiting such a unique detailed structure of 60 GHz propagations, in this section we propose a new reconstruction algorithm, namely, cluster-sparse compressed sensing (CS-CS) which is then utilized to efficiently address the channel estimations in 60 GHz millimeter-wave communications (for both LOS and NLOS cases).

3.1 Intra-cluster sparsity

The work of Li et al. in [11] suggests a novel cluster identification algorithm, and it can produce reasonable clustering results in more universal propagation environments. The cluster identification can help us achieve the scheme of cluster-classification compressed sensing.

Here, we consider the case of sparse vectors $\mathbf{x}$, i.e., $\mathbf{x}$ has only a few nonzero entries relative to its dimension. The standard sparsity model considered in compressed sensing, assumes that $\mathbf{x}$ has at most k nonzero elements, which can appear anywhere in the vector. As discussed in [12], there are practical scenarios that involve vectors $\mathbf{x}$ with nonzero entries appearing in blocks (or clusters) rather than being arbitrarily spread throughout the vector. Specific examples include signals that lie in unions of subspaces and multi-band signals [12].

The clustered sparse signals have nonzero coefficients occurring in clusters and can be represented as follows:

$$y = \Phi x, \tag{9}$$

where $\Phi \in R^{m \times N}$ denotes the measurement matrix, and the precondition is $m < N$, y represents the received signal, and x denotes the clustered sparse signal

$$x = \left[x_1, \ldots x_d, x_{d+1} \ldots x_{(2d)}, \ldots x_{(N-d+1)}, \ldots x_N\right]^T, \tag{10}$$

where $N = Md$, and $x[l](l = 1, 2, \ldots M)$ is viewed as a sub-block. Clustered-sparse means nonzero coefficients occurring in only few of the sub-blocks, and K denotes the number. To simplify the problem, we assume that all $x[l]$ are isometric. Similar to Equation 3, the measurement matrix is blocked in the following way:

$$\Phi = [\Phi_1 \ldots \Phi_d, \Phi_{d+1} \ldots \Phi_{2d}, \Phi_{N-d+1} \ldots \Phi_N] \tag{11}$$

In order to exploit the first-level sparsity, i.e., the intra-cluster sparsity, the resolvable MPCs should be classified into different groups. This process is also referred as cluster identification, which has been extensively researched in the fields of ultra-wideband (UWB) channel modeling. More specifically, such pre-process is mainly designed to extract the multiple clusters involved in 60 GHz CIRs.

It has been widely recognized that clusters in CIRs are groups of MPCs having similar *larger-scale* property,

such as time of arrival or ToA, angle of arrival or AoA, and amplitude decay; nevertheless, there still is a surprising lack of agreement concerning of a cluster definition. In most existing literatures, the cluster identification is mainly premised on the time-consuming 'visual inspection' technique. Such a method may significantly rely on *subjective* assessments of analysts and become inaccurate to realistic analysis. Thus, in this paper we alternatively resort to the recently developed automatic cluster identification method proposed by Li et al. [15].

Rather than by only utilizing the PDP characteristics, this method is essentially based on a discontinuity analysis which is generally introduced by different clusters. In order to reinforce cluster breakpoints, a nonlinear moving average ratio is firstly introduced on CIRs. Then by exploiting the wavelet analysis, a computationally efficient cluster extraction scheme is finally developed.

It is easily understood that the sparsity can be observed from the intra-cluster level; i.e., the identified clusters are also sparse in 60 GHz propagations. Thus, the cluster sparsity-based channel response for 60 GHz millimeter-wave communication systems may be expressed as follows:

$$\begin{aligned}\mathbf{x} &= \left[\mathbf{x}_{c,1}, \mathbf{x}_{c,2}, \cdots, \mathbf{x}_{c,L}\right]^T \\ &= \left[x_1, \ldots x_d, x_{d+1} \ldots x_{(2d)}, \ldots x_{(N-d+1)}, \ldots x_N\right]^T,\end{aligned} \tag{12}$$

where each group components $\mathbf{x}_{c,l}$ denotes the identified MPCs sub-vector belonging to a single cluster. To simplify the channel estimations in 60 GHz communications, we may further assume that all $\mathbf{x}_{c,l}$ (l = 1,2,..., M) are isometric; i.e., each component $\mathbf{x}_{c,l}$ has the same length d ($N = L \times d$). Despite for analysis simplicity, such a presumption may become valid by partitioning each cluster into a group of non-overlapped regions in time axis.

3.2 CS-CS

Now we may consider the case of sparse vectors $\mathbf{x}$, in which each $\mathbf{x}_{c,l}$ has only a few nonzero entries relative to the cluster arriving time. The popular sparsity modeling in CS, assuming $\mathbf{x}$ contains at most K nonzero elements, may also appear anywhere in the vector. As discussed in [16], there are also specific scenarios (e.g., the channel estimation of 60 GHz cluster-based propagations), where the vectors $\mathbf{x}$ involve nonzero entries only in some blocks (or clusters) rather than being arbitrarily spread throughout the whole vector [17]. There may exist plenty of other specific examples such as multi-band signals and signals appearing in clusters. Such a block sparsity characteristic, embodied by inner-clusters MPCs, can be properly employed to further design a more efficient channel estimation algorithm with a much lower complexity.

The clustered sparse signals may have nonzero coefficients occurring in clusters and can be represented as follows:

$$\mathbf{y} = \mathbf{\Phi}\left[\mathbf{x}_{c,1}, \mathbf{x}_{c,2}, \ldots, \mathbf{x}_{c,L}\right]^T, \tag{13}$$

where $\mathbf{\Phi} \in R^{m \times N}$ denotes the measurement matrix, and the precondition is $m < N$; $\mathbf{y}$ represents the received signal, and $\mathbf{x}$ denotes the clustered sparse signal. Here clustered-sparse means nonzero coefficients occurring in only few of the sub-blocks, $\mathbf{x}_{c,l}$ (l = 1,2,...,M), can be viewed as a sub-block which L denotes the blocks number. Accordingly, the measurement matrix $\mathbf{\Phi}$ = $[\mathbf{\Phi}_{c,1}, \mathbf{\Phi}_{c,2}, \ldots, \mathbf{\Phi}_{c,l}]$ also becomes blocked in the following:

$$\mathbf{\Phi} = [\Phi_1 \ldots \Phi_d, \Phi_{d+1} \ldots \Phi_{2d}, \ldots \Phi_{N-d+1} \ldots \Phi_N] \tag{14}$$

In fact, a lot of sparse signals may satisfy the form of block-sparse signal in practice, such as multi-band signal, DNA array (DNA microarray), radar pulse signal, and multiple measurement vector problems [16]. In addition, the reconstruction algorithm study of such sparse signal with specific structure is of great significance to many realistic problems.

3.3 Cluster-sparse compressed sensing

Based on the two-level sparsity, i.e., inter-cluster and intra-cluster, the schematic diagram of the CS-CS-based channel estimation algorithm for 60 GHz millimeter-wave communication has been shown in Figure 3. Based on such an efficient CS framework, the gain and delay of a group of resolvable multipath may be estimated blindly, that is, the pilot symbols are not necessary to the perfect reconstruction of multipath channel [18].

In order to ensure high precision of the reconstruction of a group of high-energy multipath gain and delay, the proposed cluster-based block sparsity is considered in this investigation. Based on the promising formulation of block sparsity, a new cluster sparsity-based

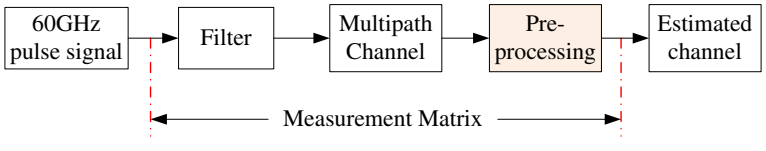

Figure 3 Block diagram for the channel estimation process based on CS.

compressed sensing algorithm (i.e., CS-CS) is introduced to the reconstruction algorithm.

The flow of the proposed channel estimation algorithm based on CS-CS has been shown by Table 1. The automatic cluster extraction algorithm proposed in [17] is used to further enhance the cluster identification performance. Such an automatic algorithm can usually produce reasonable clustering results in some more universal propagation environments. The cluster identification is employed by step A to significantly facilitate the analysis of cluster sparsity, which serves as the foundation of the new CS-CS-based channel estimation algorithm.

With regards to the above channel estimation algorithm, two important points should be noted. First, as has been suggested, since the energy of the first MPC (or first cluster) is significantly higher than the other following MPCs in subsequent cluster, the reconstruction error should be carefully controlled which may dramatically affect the whole reconstruction error. So during the proposed channel estimation algorithm, after the iterations, we may derive only one recovered MPC when the new CS-CS algorithm is applied to the first primary cluster (i.e., the direct wave component), which may essentially ensure the reconstruction accuracy of this resolvable MPC. Second, the number of resolvable MPCs is usually huge, which may bring great burdens in computations and realizations. In response to this challenge, we obtain the K-recovered values in parallel when the CS-CS applied to the second or remaining clusters, which aims mainly to maintain the low-complexity implementation of channel estimations.

4 Simulation conditions and results

In this section, we will evaluate the performance of our proposed CS-CS channel estimation algorithm via numerical simulations. For the purpose of comprehensive performance comparisons, the classical CS-ROMP algorithm is also employed in the experimental simulations.

In order to verify the reconstruction performance of two channel estimation schemes (i.e., CS-CS and CS-ROMP), the 60 GHz indoor channel modeling regulated by the IEEE P8.2.15 wireless personal area networks (WPAS) Working Group is adopted. In our analysis, $\mathbf{h}$ denotes the real multipath channel response, which is an $N \times 1$ vector and M of them are nonzero. The binary phase shift keying modulation is used and we configured the maximum delay spread to 100 ns and the sampling rate is M/N. A total of 100 tests (or independent CIR realizations) have been carried out to statistically derive the reconstruction error of CS-ROMP and the improved CS-CS algorithm. Notice that the cluster number is not *a priori* information for our CS-CS-based channel estimations, since it can be determined by the cluster identification process in step A. In order to ensure the accuracy of cluster identifications, the method proposed in [17] is adopted. The reconstruction error is measured by the mean squared error (MSE) between the real response and the recovered response, i.e.,

$$\mathrm{MSE}(\mathbf{h}) = \left\|\hat{\mathbf{h}} - \mathbf{h}\right\| / \|\mathbf{h}\| \tag{15}$$

As shown by Figures 4 and 5, the reconstruction results of both CS-ROMP and the developed CS-CS reconstruction algorithm have been derived with a simulation configuration of SNR = 20 dB, which respectively corresponds to the LOS case and NLOS situation. The vertical axis denotes the original path amplitude, accompanying the recovered ones by using the existing methods (e.g., CS-ROMP and OMP) and our improved algorithm. It should be noted that in both LOS and NLOS environments, the multipath channel may show

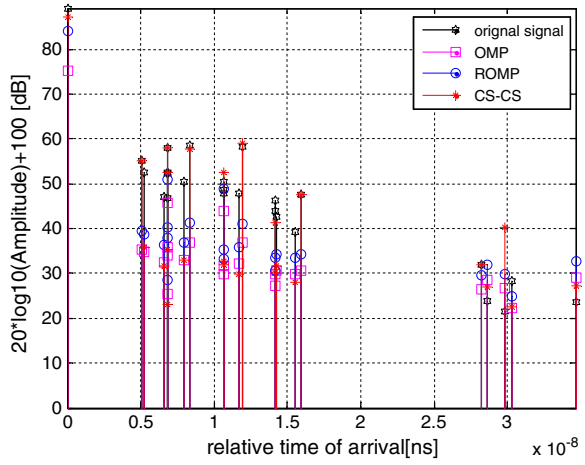

Figure 4 Channel estimation of ROMP and proposed algorithm for LOS.

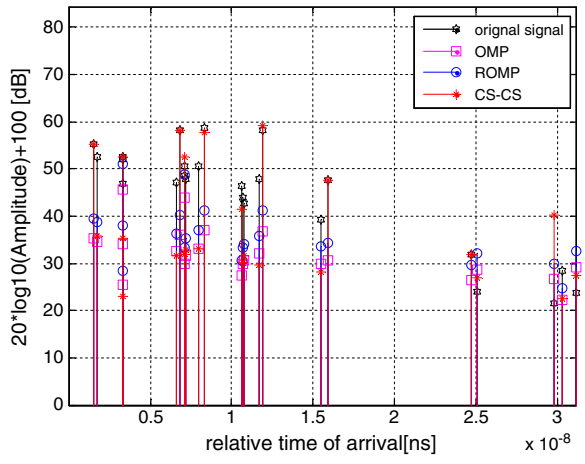

Figure 5 Channel estimation of ROMP and proposed algorithm for NLOS.

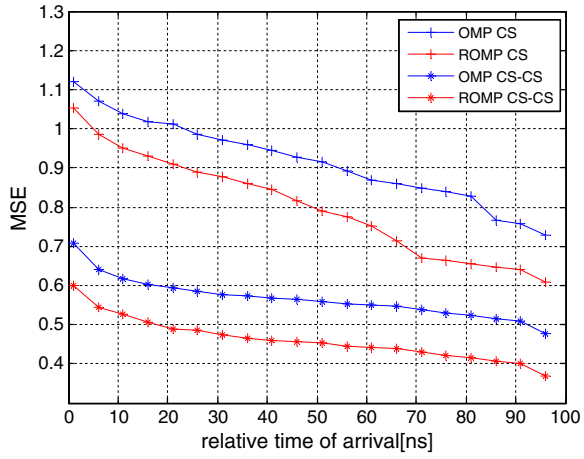

Figure 6 MSE for OMP, ROMP and proposed algorithm for LOS.

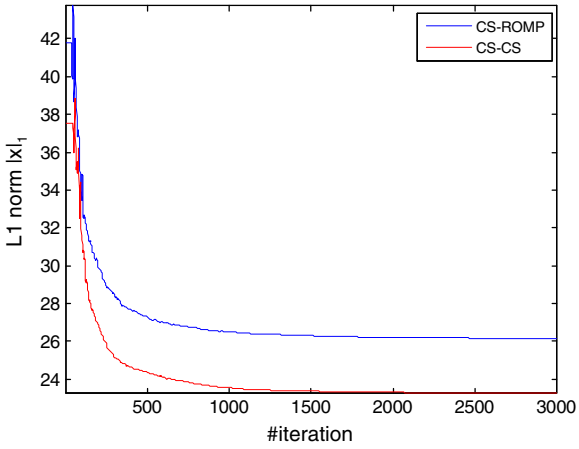

Figure 8 Iterations for CS-ROMP and proposed algorithm for LOS.

high sparsity due to the special transmission mechanics of 60 GHz millimeter-wave communication system (e.g., the large path loss and directional transmissions). From the experimental results, we may easily observe that the reconstructed response, by using the designed CS-CS algorithm, may remain perfectly in line with the first path in LOS case (or the strongest path in NLOS). Correspondingly, the performance of channel estimation of our new algorithm is also much superior to the other existing methods. For example, the more remarkable reconstruction error can be observed by using the other classical OMP or ROMP algorithms. As the main path with the highest energy has been recovered much more accurately, it may be reasonably expected that the whole reconstruction performance can be significantly improved by our presented CS-CS algorithm. Besides, it is seen that compared with the LOS channel, the deviations between the recovered paths and real ones may become much more obvious in NLOS case.

The MSE performance of channel estimations, by using CS-ROMP and CS-CS algorithm, has been demonstrated by Figures 6 and 7, respectively, for LOS and NLOS channels. For the ease of low-complexity implementation in 60 GHz receivers, we have configured the number of Rake correlation fingers to 25, that is, we mainly concentrate on the first maximum 25 rays in the performance evaluation of channel estimations. Each test will be run 100 times, and then we calculate the average reconstruction errors for each algorithm. From the simulation-derived results, we may draw the conclusion that the MSE performance of our CS-CS algorithm has been significantly improved, which properly considers the cluster characteristic of 60 GHz channels and the resulting cluster sparsity. To be specific, as shown by

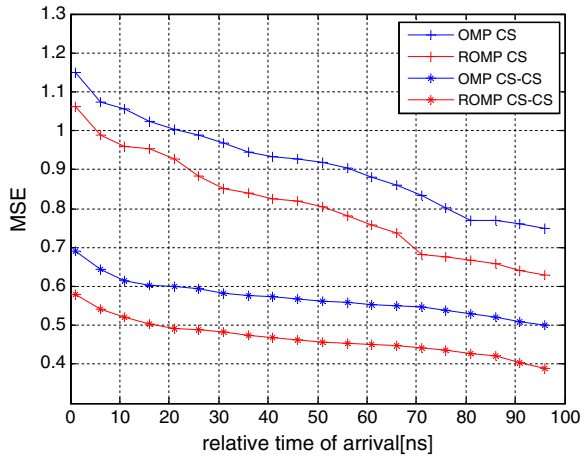

Figure 7 Bit error rate for OMP, ROMP, and proposed algorithm for NLOS.

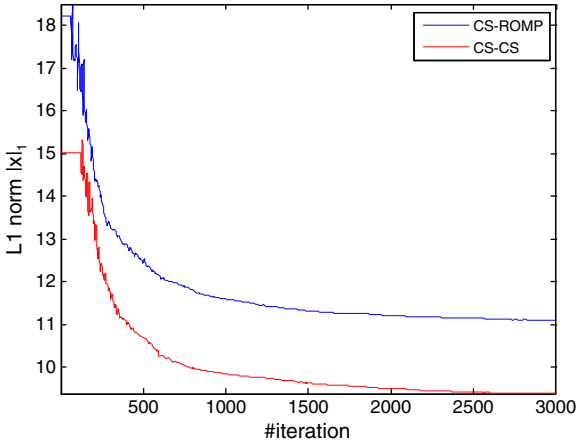

Figure 9 Iterations for CS-ROMP and proposed algorithm for NLOS.

Figure 6, the reconstruction of MSE performance in the CS-ROMP is 30% lower than that of the cluster sparsity-based CS-CS algorithm. Consequently, the precision of channel estimations can be remarkably improved.

Figures 8 and 9 have shown the iterative performance of both CS-ROMP and the proposed CS-CS algorithm in LOS and NLOS case, respectively. Due to the exploitation of block sparsity, we may see that the required iterations to reach a same error performance may be significantly reduced in our CS-CS algorithm. Taking the l_1 norm error of 27 for example, the iteration times of our new algorithm is about 200. In sharp contrast, however, the desired iteration times of CS-ROMP may even reach 1,000. As a consequence, the time complexity of channel estimations may be reduced to some extent. Besides from both Figures 8 and 9, we may also note that the convergence of the CS-CS algorithm seems to be much faster in LOS channels.

5 Conclusions

In this investigation, the structural detail or block sparsity of 60 GHz channels has been properly exploited and a promising CS-CS algorithm is designed to perform channel estimations. The other existing CS methods, i.e., CS-OMP and CS-ROMP, are also analyzed and compared with our new algorithm. The provided extensive experimental simulations, both for LOS and NLOS cases, have comprehensively demonstrated the superiority of the presented CS-CS algorithm. Based on the block sparsity that is particularly embodied by the involved multiple clusters, the designed new algorithm may produce more competitive reconstruction results. Except for the significantly reduced reconstruction errors, our method may also require a noticeably shortened iteration time compared with the existing methods, and hence, the time complexity may be reduced to some extent in the realistic channel estimation applications. It is expected that our method can be further extended to a much wider applications where the block sparsity is practically available, by efficiently reinforcing the CS reconstruction performance.

Competing interests
The authors declare that they have no competing interests.

Acknowledgments
This research is supported by the Fundamental Research Funds for the Central Universities (2012RC0103), National Natural Science Foundation of China (60902046, 60972079, 61271180), and national major special science and technology project of China (2011ZX03005-002, 2012ZX03001022). The authors also thank Dr. Bin Li for his valuable comments and discussions.

Received: 18 January 2013 Accepted: 25 March 2013
Published: 25 April 2013

References

1. HB Yang, PFM Smulders, HAJ Matti, Herben, Channel characteristics and transmission performance for various channel configurations at 60GHz. EURASIP J. Wirel. Commun. Netw. (2007). Article ID 19613
2. IEEE 802.11 WLAN very high throughput less than 6 GHz. (IEEE802.org, 2012). http://www.ieee802.org/11/-Reports/tgac_update.htm. Accessed 17 March 2012
3. IEEE 802.11 Very high throughput in 60 GHz. (IEEE802.org, 2012). http://www.ieee802.org/11/Reports/tgad_update.htm Accessed 11 March 2012
4. SK Yong, TG3c Channel modeling sub-committee final report. IEEE802.15-07-0584-01-003c (2007)
5. Y Shoji, H Sawada, CS Choi, H Ogawa, A modified S-V model suitable for line-of-sight desktop usage of millimeter-wave WPAN systems. IEEE Trans. Antennas. Propagation **57**(10), 2940–2948 (2009)
6. DL Donoho, Compressed sensing. IEEE Trans. on Inf. Theory **52**(4), 1289–1306 (April 2006)
7. SF Cotter, BD Rao, K Engan, K Kreutz-Delgado, Sparse solutions to linear inverse problems with multiple measurement vectors. IEEE Trans. Signal Process. **53**(7), 2477–2488 (2005)
8. J Chen, X Huo, Theoretical results on sparse representations of multiple-measurement vectors. IEEE Trans. Signal Process **54**(no. 12), 4634–4643 (2006)
9. X Hao, V Kukshya, TS Rappaport, Spatial and temporal characteristics of 60-GHz indoor channels. IEEE J on Selected Areas in Comm **20**(3), 620–630 (2002)
10. H Sawada, H Nakase, S Kato, Impulse response model for the cubicle environments at 60 GHz, in *Proceedings of IEEE 71th Vehicular Technology Conference (VTC 2010-Spring)* (Taipei, 2010). 16-19 May 2010 1–5
11. B Li, Z Zhou, D Li, S Zhai, Efficient cluster identification for measured ultra-wideband channel impulse response in vehicle cabin. Prog in Electromagnetics Reseach **117**, 121–147 (2011)
12. M Stojnic, F Parvaresh, B Hassibi, On the reconstruction of block-sparse signals with an optimal number of measurements. IEEE Trans. Signal. Process. **57**(no. 8), 3075–3085 (2009)
13. IEEE. org, 2005 IEEE 802.15, WPAN millimeter wave alternative PHY Task Group 3c (TG3c). http://www.ieee802.org/15/pub/TG3c.html Accessed 15 March 2012
14. YC Eldar, M Mishali, Robust recovery of signals from a structured union of subspaces. IEEE Trans. Inf. Theory **55**(11), 5302–5316 (2009)
15. JY Wang, C-W Pyo, C-S Sum, Z Lan, F Kojima, T Baykas, R Kimura, R Funada, H Harada, S Kato, H Sawada, I Lakkis, Robust and highly efficient beamforming procedures for 60GHz WPAN. (2008). IEEE 802.15-08-0190-00-003c
16. AAM Saleh, RA Valenzuela, A statistical model for indoor multipath propagation. IEEE J. Selected. Areas. Commun. **5**(2), 128–137 (Feb. 1987)
17. P Zhang, Z Hu, RC Qiu, BM Sadler, A compressed sensing based ultra-wideband communication system, in *Proceedings of IEEE International Conference on Communications (ICC)* (, Dresden, 2009)
18. JA Hogbom, Aperture synthesis with a nonregular distribution of interferometer baselines. Astronony. Astrophys **15**(Suppl), 417–426 (1974)

doi:10.1186/1687-1499-2013-114
Cite this article as: Sun *et al.*: 60 GHz ultra-wideband channel estimation based on a cluster sparsity compressed sensing. *EURASIP Journal on Wireless Communications and Networking* 2013 **2013**:114.